

Post-variational quantum neural networks

Po-Wei Huang^{1,2,*} and Patrick Rebentrost^{1,†}

¹Centre for Quantum Technologies, National University of Singapore, 3 Science Drive 2, Singapore 117543

²Department of Computer Science, National University of Singapore, 13 Computing Drive, Singapore 117417

(Dated: July 21, 2023)

Quantum computing has the potential to provide substantial computational advantages over current state-of-the-art classical supercomputers. However, current hardware is not advanced enough to execute fault-tolerant quantum algorithms. An alternative of using hybrid quantum-classical computing with variational algorithms can exhibit barren plateau issues, causing slow convergence of gradient-based optimization techniques. In this paper, we discuss “*post-variational strategies*”, which shift tunable parameters from the quantum computer to the classical computer, opting for ensemble strategies when optimizing quantum models. We discuss various strategies and design principles for constructing individual quantum circuits, where the resulting ensembles can be optimized with convex programming. Further, we discuss architectural designs of post-variational quantum neural networks and analyze the propagation of estimation errors throughout such neural networks. Lastly, we show that our algorithm can be applied to real-world applications such as image classification on handwritten digits, producing a 96% classification accuracy.

I. INTRODUCTION

Variational quantum methods [1] are proposed to solve optimization problems in chemistry [2], combinatorial optimization [3] and machine learning [4] with a potential quantum advantage in the NISQ regime [5]. These methods often use hardware-efficient Ansätze that are problem-agnostic [6]. However, many Ansätze face the well-studied barren plateau problem [7]. Several methods are suggested to alleviate this problem, including parameter initialization that form block identities [8], layerwise training [9], pretraining with classical neural networks [10], and the usage of specific architectures such as quantum convolutional neural networks [11, 12].

Partially inspired by the barren plateau problem, Huang *et al.* [13] considered the solving of linear systems with near-term quantum computers with the use of *classical combinations of quantum states* (CQS). Here, based on the input matrix, a so-called Ansatz tree is constructed which allows for a solution with provable guarantees and also for the systematic application of heuristic methods. The iterative quantum eigensolver [14] builds quantum models by assuming the model to be a linear combination of unitaries and iteratively adding terms to the model until a close enough estimate is produced. Further, these concepts have also found use in quantum algorithms for semidefinite programming [15]. It is interesting to consider these concepts for other settings and problems such as neural networks for machine learning.

In our work, we discuss strategies that rely on the variational method of finding approximations in quantum mechanics as the theoretical basis for optimization but avoid the usage for parameterized quantum states. These strategies are part of what can be called “*post-variational*

methods”. In our post-variational methods, we take the classical combination of multiple fixed quantum circuits and find the optimal combination though solving a classical convex optimization problem. We show that our post-variational methods benefit from the much shallower and simpler construction of their quantum circuits compared to both variational and fault-tolerant algorithms. As no variational parameters are used, the barren plateau issue of vanishing gradients can be avoided. Furthermore, we show a possible reduction in quantum measurements when compared to variational algorithms as our protocol does not require the iterative update of variational algorithms and can be further reduced to one-shot random measurements when the classical shadows protocol is applied [16]. In particular, we discuss the use of classical combinations of quantum circuits regarding quantum machine learning and neural networks. While our methods can consume more quantum resources than variational algorithms, they could provide a viable alternative in the NISQ regime (Figure 1).

II. PRELIMINARIES

Notations. Given a field \mathbb{F} of either real or complex numbers, for vector $v \in \mathbb{F}^N$, we denote $\|v\|_p$ as its ℓ_p norm. Given a collection/set of scalars S over field \mathbb{F} , we can use the operation $\text{vec}(S)$ to vectorize the collection. We denote $[h]$ to be the set $\{1, 2, \dots, h\}$.

For a matrix $A \in \mathbb{F}^{M \times N}$, let A_{ij} be the (i, j) -element of A . We denote the spectral norm to be $\|A\|_2 = \max_i \sigma_i(A)$ and the max norm to be $\|A\|_{\max} = \max_{ij} |A_{ij}|$, where $\sigma_i(A)$ are singular values of A . Furthermore, we denote $\sigma_{\min}(A)$ to be the smallest non-zero singular value of A . We also denote A^+ to be the Moore-Penrose inverse of A [17]. We note that $\|A^+\|_2 = \frac{1}{\sigma_{\min}(A)}$.

Classical shadows. The classical shadows method [16] introduces a randomized protocol to estimate the value of $\text{tr}(O_i \rho)$ over M observables up to additive error ϵ with

* huangpowei22@u.nus.edu

† cqtfr@nus.edu.sg

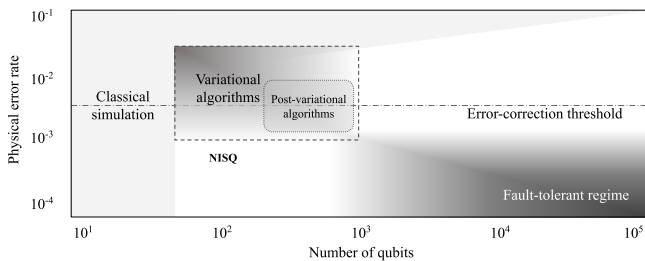


FIG. 1. A sketch of quantum algorithm regimes. The noisy intermediate quantum regime (NISQ) was defined by Preskill [5] to be a certain range for both qubit numbers and gate errors (hence a rectangle in this graphic). Regimes with only higher qubits or only lower errors are outside NISQ as the other metric (error rate or qubit number, respectively) is not sufficient to harness the additional resources. Variational algorithms are the main candidates for the NISQ regime and post-variational algorithms reside in the higher-qubit part of NISQ, but avoid barren plateaus and have certain provable guarantees. Fault-tolerant algorithms reside in a range of a large number of qubits and low errors.

$O(\log(M))$ measurements. The quantum state is first evolved by a random unitary U selected from a tomographically complete set of unitaries, i.e. $\rho \rightarrow U\rho U^\dagger$. Measuring the transformed quantum state in the computational basis, a string of outcomes $b \in \{0, 1\}^n$ can be produced. One can then construct and store $U^\dagger|b\rangle\langle b|U$ classically using the stabilizer formalism [18], the expectation of which can be viewed as a quantum channel \mathcal{M} , i.e., $\mathbb{E}[U^\dagger|b\rangle\langle b|U] = \mathcal{M}(\rho)$. By inverting the quantum channel and repeating the above process multiple times, we can obtain multiple “classical shadows” $\hat{\rho}$ of the density matrix ρ such that $\hat{\rho} = \mathcal{M}^{-1}(U^\dagger|b\rangle\langle b|U)$. These classical shadows can be used to approximate the value of the quantum state $\text{tr}(O_i\rho)$ against a series of observables O_1, O_2, \dots, O_M via the median-of-means estimator [19]. The number of classical shadows required to estimate M observables within an additive error of ϵ is $O(\log M \max_i \|O_i\|_{\text{shadow}}^2/\epsilon^2)$, where $\|O_i\|_{\text{shadow}}^2$, or the shadow norm, is dependent on the unitary ensemble used. When using tensor products of single-qubit Clifford gates (which is equivalent to measurement on a Pauli basis), $\|O_i\|_{\text{shadow}}^2 \leq 4^{\mathcal{K}} \|O_i\|_2^2$ for observable O_i that acts non-trivially on \mathcal{K} qubits. For the rest of this paper, we call this particular property of an observable to be its *locality*, and denote the shadow norm as $\|\cdot\|_S$.

Loss functions. In this paper, we also refer to a variety of different loss functions that are used in different machine learning tasks. Given d data points with ground truth $\{y_i\}_{i=1}^d$ and predicted values $\{\hat{y}_i\}_{i=1}^d$, where $\forall i, y_i, \hat{y}_i \in \mathbb{R}$, the root-mean-square error (RMSE) loss is defined as follows: $\mathcal{L}_{\text{RMSE}} = \sqrt{\frac{1}{d} \sum_{i=1}^d (y_i - \hat{y}_i)^2}$, while the mean absolute error (MAE) loss is defined by $\mathcal{L}_{\text{MAE}} = \frac{1}{d} \sum_{i=1}^d |y_i - \hat{y}_i|$. In the case where the ground truth is binary, i.e. $\forall i, y_i \in \{0, 1\}$ and predictions $\hat{y}_i \in [0, 1]$, the binary cross-entropy (BCE) loss is defined

as $\mathcal{L}_{\text{BCE}} = \frac{1}{d} \sum_{i=1}^d -y_i \log(\hat{y}_i) - (1 - y_i) \log(1 - \hat{y}_i)$.

Furthermore, given $A \in \mathbb{C}^{N \times N}$, $b \in \mathbb{C}^N$, we have a task to find a solution vector $x \in \mathbb{C}^N$ for linear system $Ax = b$ with quantum computation. Constructing estimator \hat{x} of x , one can define the Hamiltonian loss as $\langle \hat{x} | A^\dagger (\mathbb{I} - |b\rangle\langle b|) A | \hat{x} \rangle$. [13, 20]

III. THE POST-VARIATIONAL METHOD

Problem setting. We are given a dataset, $\mathcal{D} = \{(x_i, y_i)\}_{i=1}^d$, where d is the number of data, the feature vectors are $x_i \in \mathbb{R}^\ell$, with ℓ being the number of features, and the labels $y_i \in \mathbb{R}$. Our task is to learn an estimator $\mathcal{E}_\vartheta(x_i)$ via parameterized neural networks with parameters ϑ that make use of quantum circuits such that $\hat{y}_i := \mathcal{E}_\vartheta(x_i)$. We aim to minimize the difference between the estimator \hat{y}_i and ground truth y_i over all data with a given loss function \mathcal{L} .

Variational methods. Variational quantum algorithms have been regarded as the analogue to neural networks in quantum systems, and are also referred to as quantum neural networks (QNNs) when applied to machine learning tasks. Referring to a class of circuit-centric variational quantum algorithms operating on pure states [21, 22], such algorithms operate by first encoding data x into a n -qubit quantum state $\rho(x) \in \mathbb{C}^{2^n \times 2^n}$. The quantum state is then transformed by an Ansatz $U(\theta)$, with parameters $\theta \in \mathbb{R}^k$, to form a trial quantum state

$$\rho_{\text{trial}}(\theta, x) = U(\theta)\rho(x)U^\dagger(\theta). \quad (1)$$

We can then construct the estimator with an observable O such that

$$\mathcal{E}_\theta(x) := \text{tr}(O\rho_{\text{trial}}(\theta, x)). \quad (2)$$

The parameters θ are optimized by evaluating gradients of the quantum circuit via parameter-shift rules [4, 23] and calculating updates of the parameter via gradient-based optimization on classical computers.

Apart from the simple construction of variational algorithms stated above that uses a single layer of data encoding followed by a variational Ansatz, there are variational algorithms make use of alternating data encoding layers and parameterized Ansätze, also known as data re-uploading models [24]. Such models are shown to have an exact mapping to the simpler construction of variational algorithms as shown above [25], albeit with an exponential increase of qubits. In our work, as we do not specify the data encoding layer, we discuss the simpler construction by Schuld *et al.* [21] as a general structure that encompasses the mapped versions of data re-uploading models as well.

The post-variational method. Inspired by the CQS approach [13], we propose two *post-variational methods* and a hybrid version of them. For the first method, we take classical combinations of various fixed quantum Ansätze in replacement of a single parameterized Ansatz.

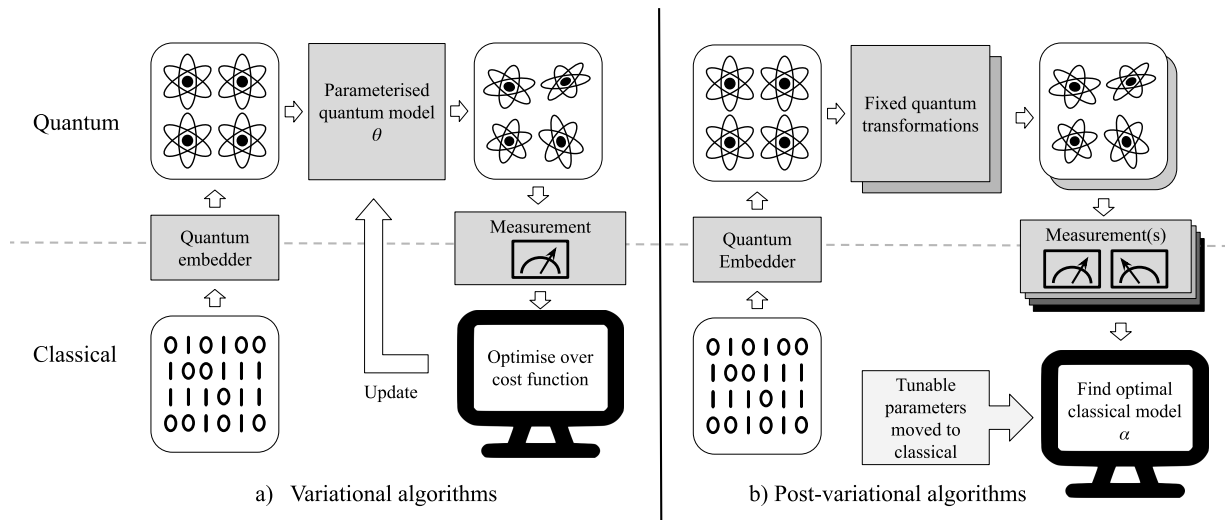


FIG. 2. High-level sketch of post-variational strategies for near-term quantum computing. The variational method uses parameterized quantum circuits to transform embedded input data before suitable measurements, see panel a). Post-variational methods, see panel b), use multiple fixed circuits, which may share similar circuit structure as the variational circuits, and multiple measurements of these circuits. The goal is to achieve approximately similar accuracy as the variational methods, while only performing optimization of classical parameters and retaining the power of quantum embeddings.

For the second method, this idea can be generalized to *classical combinations of quantum observables* (CQO) by combining the Ansatz $U(\theta)$ and observable O into a single parameterized observable $\mathcal{O}(\theta)$ and replacing this observable with a collection of predefined trial observables $\mathcal{O}_1, \mathcal{O}_2, \dots, \mathcal{O}_m$. For both cases, measurement results on the quantum circuits are then combined classically, where the optimal weights of each measurement is computed via classical neural networks over a convex optimization problem. See Figure 2 for a high-level sketch of the idea behind post-variational methods.

Classical combinations of quantum observables. Starting from our variational observable O , we can combine the parameterized Ansatz with the observable to obtain a parameterized observable $\mathcal{O}(\theta) := U^\dagger(\theta)OU(\theta)$. The expectation values are the same as $\text{tr}(O\rho_{\text{trial}}(\theta, x)) = \text{tr}(\mathcal{O}(\theta)\rho(x))$. Therefore, instead of optimizing over parameterized trial quantum states, we can optimize over a parameterized observable to achieve the same effect. As any observable can be expressed as a linear combination of Hermitians, one can express the observable $\mathcal{O}(\theta)$ as linear combinations weighted by functions $\mathcal{F}_j: \mathbb{R}^k \rightarrow \mathbb{R}$ of θ such that

$$\mathcal{O}(\theta) = \sum_{j=1}^M \mathcal{F}_j(\theta)\mathcal{O}_j, \quad (3)$$

where M is upper bounded by 4^n . We leave the construction of such decompositions to Appendix A.

Noting that the estimator can be written as follows, $\mathcal{E}_\theta(x) = \text{tr}(\mathcal{O}(\theta)\rho(x)) = \sum_{j=1}^M \mathcal{F}_j(\theta) \text{tr}(\mathcal{O}_j\rho(x))$, we can model such systems by considering the entire system as a function $\mathcal{H}: \mathbb{R}^k \times \mathbb{R}^M \rightarrow \mathbb{R}$ of θ and the M terms of

$\text{tr}(\mathcal{O}_j\rho(x))$ such that

$$\mathcal{E}_\theta(x) = \mathcal{H}_\theta(\text{vec}(\{\text{tr}(\mathcal{O}_j\rho(x))\}_{j=1}^M)). \quad (4)$$

By universal approximation theorem [26], we can approximate function \mathcal{H}_θ classically through neural network model \mathcal{G}_α parameterized by classical parameters α , such that

$$\mathcal{E}_\theta(x) \approx \mathcal{G}_\alpha(\text{vec}(\{\text{tr}(\mathcal{O}_j\rho(x))\}_{j=1}^M)) = \mathcal{E}_\alpha(x). \quad (5)$$

Under this framework, the estimator can be further extended to simulate non-linear systems.

In simple linear cases, a concrete procedure for creating classical combinations of quantum observables is as follows. Make a first approximation (I) and consider only a subset \mathcal{S} of size $|\mathcal{S}| = m$ of the trial observables. This leads to

$$\mathcal{O}(\theta) \approx \sum_{j:\mathcal{O}_j \in \mathcal{S}} \mathcal{F}_j(\theta)\mathcal{O}_j. \quad (6)$$

We then make our second approximation (II) and consider all the functions independently. Each function $\mathcal{F}_j(\theta)$ is considered as a classical parameter $\alpha_j \in \mathbb{R}$. This leads to

$$\mathcal{O}(\theta) \rightarrow \mathcal{O}(\alpha) := \sum_{j:\mathcal{O}_j \in \mathcal{S}} \alpha_j \mathcal{O}_j. \quad (7)$$

Hence, we obtain a linear combination of observables, which, assuming the approximations are chosen judiciously, will contain much of the initial complexity.

Comparisons with CQS. The CQS approach [13] was originally proposed to solve linear systems of equations of $Ax = b$, where the solution of x can be found by taking the Moore-Penrose inverse of A such that $x = A^+b$. With the variational approach, A^+ is modeled by a variational Ansatz $U(\theta)$, while the CQS approach takes classical combinations of fixed ‘‘problem-inspired’’ Ansätze $U_1, U_2, \dots, U_{m_{\text{CQS}}}$ generated by the matrix A in conjunction with an Ansatz tree. An estimator \hat{A}^+ of A^+ is constructed such that $\hat{A}^+ = \sum_{i'=1}^{m_{\text{CQS}}} \gamma_{i'} U_{i'}$, where $\gamma_i \in \mathbb{R}_{>0}$.

We note that the CQS approach can be viewed as a problem-inspired analogue to the post-variational method when viewing the problem under the Hamiltonian loss as opposed to the MSE loss used by Huang *et al.* [13]. In particular, we see that the loss term can be formulated as follows:

$$\begin{aligned} \mathcal{L}_{\text{Hamiltonian, CQS}} &= \text{tr} \left(\left(\sum_{i'=1}^{m_{\text{CQS}}} \gamma_{i'} U_{i'}^\dagger \right) O \left(\sum_{j'=1}^{m_{\text{CQS}}} \gamma_{j'} U_{j'} \right) |b\rangle\langle b| \right) \quad (8) \\ &= \sum_{i'=1}^{m_{\text{CQS}}} \gamma_{i'}^2 \text{tr}(U_{i'}^\dagger O U_{i'} |b\rangle\langle b|) \\ &\quad + \sum_{i'=1}^{m_{\text{CQS}}} \sum_{j' \neq i'} \gamma_{i'} \gamma_{j'} \text{tr} \left(\frac{(U_{i'}^\dagger O U_{j'}) + (U_{j'}^\dagger O U_{i'})}{2} |b\rangle\langle b| \right), \quad (9) \end{aligned}$$

where $O = A^\dagger(\mathbb{I} - |b\rangle\langle b|)A$.

Collecting the terms and corresponding coefficients of $U_{i'}^\dagger O U_{i'}$ and $\frac{1}{2}((U_{i'}^\dagger O U_{j'}) + (U_{j'}^\dagger O U_{i'}))$ into predefined trial observables \mathcal{O}_j and their corresponding coefficients $\alpha_j \in \mathbb{R}$, we find that we can write the Hamiltonian loss of the CQS approach as the mean-absolute error (MAE) loss of the post-variational approach as

$$\mathcal{L}_{\text{Hamiltonian, CQS}} = \sum_{j=1}^m \alpha_j \text{tr}(\mathcal{O}_j |b\rangle\langle b|) \quad (10)$$

$$= \left| 0 - \sum_{i=1}^m \alpha_i \text{tr}(\mathcal{O}_i |b\rangle\langle b|) \right| \quad (11)$$

$$= \mathcal{L}_{\text{MAE, Post-Variational}} \quad (12)$$

where we note that 0 serves as the ground truth of the MAE loss as $\langle x|A^\dagger(\mathbb{I} - |b\rangle\langle b|)A|x\rangle = 0$. Here, $m = m_{\text{CQS}}^2$ by counting the different terms.

IV. DESIGN PRINCIPLES OF POST-VARIATIONAL QUANTUM CIRCUITS

We now discuss multiple possible heuristic strategies to decide on the trial observables \mathcal{O}_j and construct the circuits for our post-variational algorithm to minimize operations on quantum computers. See Figure 3 for an

overview of the heuristic strategies. Recall that we construct a post-variational algorithm by ensembling multiple trial observables such that the final target observable can be learned by combination of the measurement results based on a learned function:

$$\mathcal{E}_\theta(x) \approx \mathcal{E}_\alpha(x) = \mathcal{G}_\alpha(\text{vec}(\{\text{tr}(\mathcal{O}_j \rho(x))\}_{j:\mathcal{O}_j \in \mathcal{S}})), \quad (13)$$

where for linear cases

$$\mathcal{G}_\alpha(\text{vec}(\{\text{tr}(\mathcal{O}_j \rho(x))\}_{j:\mathcal{O}_j \in \mathcal{S}})) = \sum_{j:\mathcal{O}_j \in \mathcal{S}} \alpha_j \text{tr}(\mathcal{O}_j \rho(x)). \quad (14)$$

Ansatz expansion. The first strategy to constructing post-variational algorithms is to first begin with a variational algorithm and replace the parameterized Ansatz $U(\theta)$ with an ensemble of p fixed Ansätze $\{U_a\}_{a=1}^p$. Huang *et al.* [13]’s CQS approach uses this strategy to solve linear systems, generating the fixed problem-inspired Ansätze through the usage of an Ansatz tree.

For quantum machine learning tasks, such problem-inspired Ansätze may not be readily available, hence we generate the fixed Ansätze from a problem-agnostic Ansatz. Starting from the initialized parameters $\theta^{(0)}$ of a parameterized Ansatz $U(\theta)$, we can perform Taylor expansion of the Ansatz at $\theta^{(0)}$ such that

$$\begin{aligned} U(\theta) &= U(\theta^{(0)}) + \sum_{u=1}^k \Delta\theta(\partial_{\theta_u} U)(\theta^{(0)}) \\ &\quad + \sum_{u=1}^k \sum_{v=1}^k \frac{1}{2!} \Delta\theta_u \Delta\theta_v (\partial_{\theta_u} \partial_{\theta_v} U)(\theta^{(0)}) + \dots, \quad (15) \end{aligned}$$

and combine the gradient, Hessian, and higher-order derivatives of the original Ansatz classically. See Figure 4 for a representation of such quantum circuits.

For implementations on quantum hardware, it may be difficult to take the direct expansion of the Ansatz itself, hence we instead take the derivatives of the parameterized observable $\mathcal{O}(\theta)$ via parameter-shift rules [4, 23], which can also be extended to derivatives of higher-orders [27, 28]. However, the order of derivatives we can take is limited as the number of quantum circuits required to obtain high-order derivative via parameter-shift rules scale exponentially with the order of the derivative.

Note that if the initial parameter $\theta^{(0)}$ falls within a barren plateau, taking higher-order derivatives do not help with the escape from the barren plateau [29], hence we rely instead on suitable initializations of $\theta^{(0)}$ to avoid such problems [8]. Such initializations guarantee non-triviality of gradients at the initial point and can be extended to higher-order derivative, allowing such strategies to be more useful in the post-variational setting rather than variational settings, as such guarantees cannot be extended to later stages of the gradient descent process.

Observable construction. In contrast to the Ansatz expansion strategy, where we generate fixed Ansätze either through Ansatz trees or Taylor expansions, in the

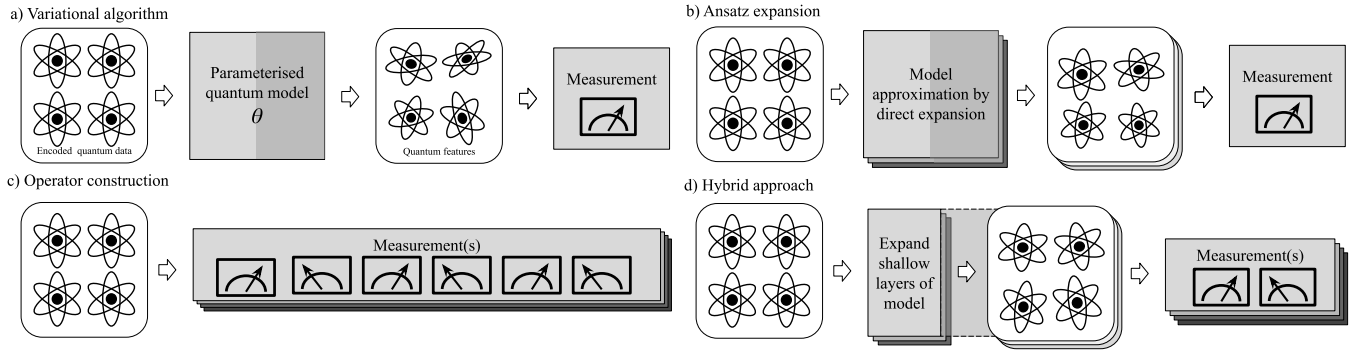


FIG. 3. Here we provide an overview of the various strategies introduced in the later text. Using the variational circuit (a) as a baseline, the Ansatz expansion approach (b) does model approximation by directly expanding the parameterized Ansatz into an ensemble of fixed Ansatzes. On the other hand, the observable construction approach (c) foregoes all usage of an Ansatz and directly constructs a measurement observable by ensembling and taking the classical combination of various predefined trial observables. The hybrid approach (d) does both the expansion of the Ansatz, albeit only on the shallower layer of the model, and replacing the deeper layers of the model as well as the measurement observable with a series of measurement trial observables that can be used to retrieve a classical combination.

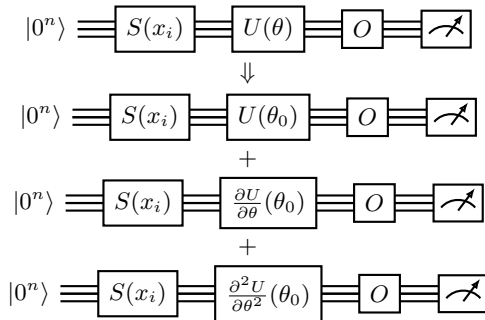


FIG. 4. Ansatz expansion approach to post-variational algorithm construction. Starting from a variational Ansatz, multiple non-parameterized quantum circuits are constructed by Taylor expansion of the Ansatz around a suitably chosen initial setting of the parameters θ_0 . The different circuits are linearly combined with classical coefficients that are optimized via convex optimization.

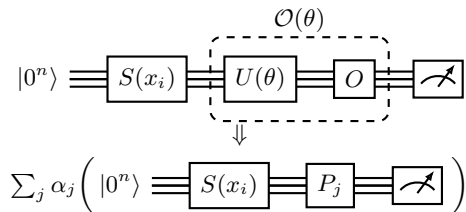


FIG. 5. Observable construction approach to post-variational algorithm construction. A variational observable can be directly constructed by an ensemble of Pauli observables, and may serve as a potential approximation under locality restrictions.

observable construction strategy, we take the CQO strategy discussed in the previous section at face value, decomposing the parameterized observable $\mathcal{O}(\theta)$ against the basis of quantum observables (namely, Paulis), such

that $\mathcal{O}(\theta) \rightarrow \mathcal{O}(\alpha) = \sum_{P \in \{\mathcal{I}, \mathcal{X}, \mathcal{Y}, \mathcal{Z}\}^{\otimes n}} \alpha_P P$. See Figure 5 for a representation of such quantum circuits.

However, such a method scales exponentially with the number of qubits used in the system, creating an analogue to the barren plateau. Further heuristic selections of observables would be required to prevent such exponential scalings. We find that considering all Pauli observables within a certain locality \mathcal{K} as a good heuristic given that most physical Hamiltonians are local. Furthermore, recent work by Huang *et al.* [30] show that this truncation by locality of Pauli observables, which they refer to as “low-weight approximations”, is proven to be a good surrogate for the unknown observable-to-be-learned under the circumstance that the quantum state ρ that the observable is applied to is sampled from distributions that are invariant under single-Clifford gates. They further show that these low-weight approximations would require only a quasi-polynomial number of samples in relation to the number of qubits n to learn.

Under the circumstance that the target observable \mathcal{O} is \mathcal{K} -local, we can employ the classical shadows protocol [16] to reduce the quantum measurements needed on the quantum computer while achieving the same additive error term ϵ determined by the loss term. For each data sample x such that we can prepare a quantum state $\rho(x)$, we can obtain a series of classical shadows of the quantum state $\hat{\rho}(x)$ that can be stored classically such that we can estimate the values of $\text{tr}(P\rho(x))$ where $P \in \{\mathcal{I}, \mathcal{X}, \mathcal{Y}, \mathcal{Z}\}^{\otimes n} : |P| \leq \mathcal{K}$. The classical shadows protocol is able to reduce the number of measurements required for all values for $\text{tr}(P\rho(x))$ from a polynomial dependency of the number of qubits to a logarithmic dependency. We discuss this further in Section VI.

The hybrid strategy. When taking the strategy of observable construction, one may additionally want to use parameterized Ansatz quantum circuits. Hence, we discuss a simple hybrid strategy that combines both the

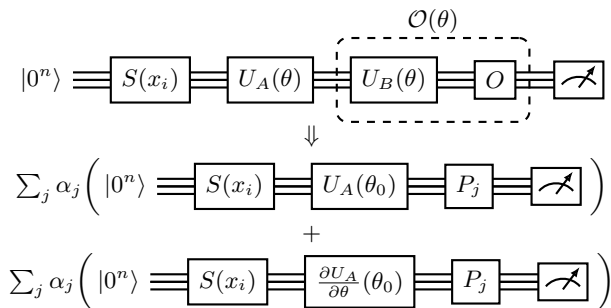


FIG. 6. Hybrid approach to post-variational algorithm construction. This approach is a combination of the approaches shown in Figures 4 and 5.

usage of Ansatz expansion and observable construction. See Figure 6 for a representation of such quantum circuits.

Recall the definition of the parameterized observable as $\mathcal{O}(\theta) = U(\theta)OU^\dagger(\theta)$. Instead of expanding $U(\theta)$ directly, we split the Ansatz $U(\theta)$ into two unitaries (based on cutting the circuit at a certain depth, for example), such that $U(\theta) = U_A(\theta_A)U_B(\theta_B)$. We can now write $\mathcal{O}(\theta) = U_A(\theta_A)U_B(\theta_B)OU_B^\dagger(\theta_B)U_A^\dagger(\theta_A)$. We denote $\mathcal{O}'(\theta_B) = U_B(\theta_B)OU_B^\dagger(\theta_B)$. Using the observable construction approach applied to $\mathcal{O}'(\theta_B)$ and Ansatz expansion applied to $U_A(\theta_A)$, we can lower the depth of the circuit to minimize complexity and barren plateaus, while keeping enough of the Ansatz to retain problem-related design advantages as well as the ability to approximate variational models that act globally on all qubits.

We note that barren plateaus occur in shallow Ansätze if the observable employed in variational algorithms is global [31]. Due to the evaluated results of the derivative of the Ansätze measured on global observables being small trivial values that vanish exponentially in relation to the total number of qubits n , we can directly prune such measurements and only use local observables to approximate $\mathcal{O}'(\theta_B)$. With the observables used restricted to local observables, we can once again employ the classical shadows method to reduce measurements.

V. ARCHITECTURE DESIGN OF POST-VARIATIONAL NEURAL NETWORKS

Let it be possible to approximate the target observable $\mathcal{O}(\theta)$ obtained in a variational algorithm with a predefined collection of trial observables $\mathcal{S} = \{\mathcal{O}_1, \mathcal{O}_2, \dots, \mathcal{O}_m\}$, such that $\mathcal{E}_\theta(x) = \text{tr}(\mathcal{O}(\theta)\rho(x)) \approx \sum_{j: \mathcal{O}_j \in \mathcal{S}} \alpha_j \text{tr}(\mathcal{O}_j\rho(x))$. Then the optimal values of the coefficients $\alpha_1, \alpha_2, \dots, \alpha_m$ are found with classical optimization by perceptrons or neural networks. Following the idea of neural networks, we call each individual quantum circuit as a quantum neuron [32].

Definition V.1. We define a (p, q) -hybrid strategy as

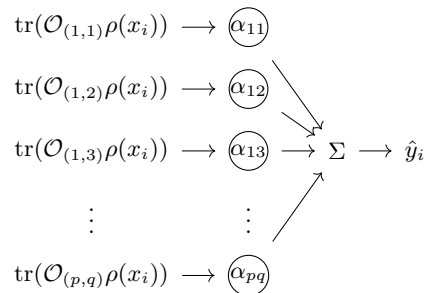


FIG. 7. Classical linear regression approach of the hybrid model for a (p, q) -hybrid strategy. Given a set of operators $\mathcal{O}_{(i,j)}$, $i \in [p]$ and $j \in [q]$, and data embedding $\rho(x)$, a simple linear quantum neural can be constructed by combining the outputs in a linear fashion using combination parameters α_{ij} . This obtains the output label \hat{y} .

a strategy with a total of p Ansätze $\{U_a\}_{a=1}^p$ and q observables $\{O_b\}_{b=1}^q$, such that the output of each circuit for any input ρ is $\text{tr}(\mathcal{O}_{(a,b)}\rho) = \text{tr}(U_a^\dagger O_b U_a \rho)$.

As the outcome of quantum neuron measurements are probabilistic, multiple measurements need to be conducted in order to produce a good estimate. We refer to each quantum circuit that employs the fixed Ansatz and observable as a quantum neuron.

We define matrix $Q \in \mathbb{R}^{d \times m}$ such that

$$Q_{ij} := \text{tr}(\mathcal{O}_j\rho(x_i)), \quad (16)$$

where $\{\mathcal{O}_j\}_{j=1}^m$ is the collection of observables produced by a (p, q) -hybrid strategy and $m = pq$. We use Q as the input to a classical linear regression model (Figure 7). We minimize the root-mean-square error as follows

$$\mathcal{L}_{\text{RMSE}} = \sqrt{\frac{1}{d} \sum_{i=1}^d \left(y_i - \sum_{a=1}^p \sum_{b=1}^q \alpha_{a,b} \text{tr}(\mathcal{O}_{(a,b)}\rho(x_i)) \right)^2} \quad (17)$$

$$= \frac{1}{\sqrt{d}} \|Y - Q\alpha\|_2, \quad (18)$$

where $Y = (y_1, y_2, \dots, y_d)^\top$. The closed form solution to solving linear regression problems obtains $\alpha = Q^+Y$, or in the special case where Q has full column rank and thus $Q^\top Q$ is positive definite, we obtain $\alpha = (Q^\top Q)^{-1}Q^\top Y$.

Here, we use a simple linear regression model as the main classical model. However, this model can be extended to any classical model including feed-forward models; we only mention linear regression models in detail for easy analysis with closed-form solutions. Furthermore, the results can be extended to classification problems by adding an extra sigmoid or softmax function at the end of the output.

VI. ERROR ANALYSIS OF POST-VARIATIONAL NEURAL NETWORKS

Given the design of post-variational neural networks based on a simple linear regression model as the classical ensemble model for quantum neurons. Measurement outcomes in quantum systems are probabilistic, and hence estimated quantities come with errors that may be carried and propagated throughout the entire neural network system. In this section, we discuss the effects of such errors as well as the number of measurements required to achieve a target final error.

Estimation errors. We first show the simple result for the total number of measurement for all terms $\text{tr}(\mathcal{O}_{(a,b)}\rho(x_i))$.

Proposition VI.1 (Measurements needed for direct estimation of all quantum neurons). *Consider a (p, q) -hybrid strategy as in Definition V.1. Using the sample mean over multiple iterations as an estimator to evaluate the output of each of the $m = pq$ quantum neurons, the number of quantum measurements required to estimate the output of all quantum neurons over all d data points such that the all $m \times d$ outputs have an additive error of ϵ_H with a probability of $1 - \delta$ falls within*

$$O\left(\frac{md}{\epsilon_H^2} \log \frac{md}{\delta}\right).$$

The proof is an application of Hoeffding [33] and union bound [34] and is shown in Appendix B. Alternatively, one can reduce the number of total measurements by estimating the output of all quantum neurons that contain the same fixed Ansatz over a single data point by utilizing the classical shadows protocol.

Proposition VI.2 (Measurements needed for shadow estimation of all quantum neurons). *Consider a (p, q) -hybrid strategy as in Definition V.1. Using the classical shadows to estimate output of all $m = pq$ quantum neuron over all d data points, the number of quantum measurements required such that the all $m \times d$ outputs have an additive error of ϵ_H with a probability of $1 - \delta$ falls within*

$$O\left(\frac{pd}{\epsilon_H^2} \max_{k \in [q]} \|O_k\|_S^2 \log \frac{md}{\delta}\right).$$

The proof is via application of the bounds of the median-of-means estimator [19] and union bound [34] and is shown in Appendix B.

Relating back to the design principles, we note that the classical shadows protocol does not help with the Ansatz expansion approach as $q = 1$ and $m = p$, and instead increases the complexity by $\|O\|_S^2$. For the observable construction and hybrid approach, we now consider the case where the observables are the complete set of \mathcal{K} -local Paulis. The number of observables q is then

$$\sum_{\ell=0}^{\mathcal{K}} \binom{n}{\ell} 3^\ell \in O(3^\mathcal{K} n^\mathcal{K}). \quad (19)$$

As shown in [16], the shadow norm $\|O\|_S^2$ is upper bounded by $3^\mathcal{K}$. Hence, the total number of measurements needed for the classical shadows protocol is then

$$O\left(\frac{3^\mathcal{K} \mathcal{K} p d}{\epsilon_H^2} \log \frac{np}{\delta}\right), \quad (20)$$

a reduction from direct measurements, which take

$$O\left(\frac{3^\mathcal{K} n^\mathcal{K} \mathcal{K} p d}{\epsilon_H^2} \log \frac{np}{\delta}\right), \quad (21)$$

where n is the number of number of qubits.

Error propagation through neural networks. Recall that we define Q such that $Q_{ij} = \text{tr}(\mathcal{O}_j \rho(x_i))$ from Equation 16. Given that each element in Q is the expected outcome of a quantum neuron, we construct \hat{Q} such that \hat{Q}_{ij} is the estimated outcome of the quantum neuron that falls within an additive error of ϵ_H by multiple direct measurements in Proposition VI.1 or by utilizing classical shadow estimations in Proposition VI.2. Formally, $\forall i, j \quad |\hat{Q}_{ij} - Q_{ij}| \leq \epsilon_H$. We now consider the effect of such errors on the loss function \mathcal{L} that we use for machine learning problems.

For linear regression, we consider the RMSE loss of $\mathcal{L}_{\text{RMSE}}(\alpha, Q)$ from Equation 18. We then define the following optimal parameters α^* and $\hat{\alpha}^*$, for Q and \hat{Q} , respectively, where

$$\alpha^* := \arg \min_{\alpha} \mathcal{L}_{\text{RMSE}}(\alpha, Q), \quad (22)$$

$$\hat{\alpha}^* := \arg \min_{\hat{\alpha}} \mathcal{L}_{\text{RMSE}}(\hat{\alpha}, \hat{Q}). \quad (23)$$

Further, we define using only Q ,

$$\Delta \mathcal{L}_{\text{RMSE}} := |\mathcal{L}_{\text{RMSE}}(\hat{\alpha}^*, Q) - \mathcal{L}_{\text{RMSE}}(\alpha^*, Q)|. \quad (24)$$

We then obtain the following proposition, the proof of which can be found in Appendix C.

Theorem VI.3 (Linear regression theoretical guarantee). *Consider a (p, q) -hybrid strategy as in Definition V.1, and let $m = pq$. Let Q be the matrix as defined in Equation 16. Let $\epsilon > 0$ and let \hat{Q} be such that*

$$\|\hat{Q} - Q\|_{\max} < \min\left(\frac{\min(\sigma_{\min}(Q), \sigma_{\min}(\hat{Q}))}{\sqrt{\min(m, d)md}}, \frac{\epsilon}{6\sqrt{m}\|Y\|_2\|Q\|_2\|Q^+\|_2^2}\right).$$

Then, for the loss difference as defined in Equation 24, $\Delta \mathcal{L}_{\text{RMSE}} < \epsilon$.

To find the number of measurements needed to obtain a loss difference within ϵ , we first set the provided upper bounds to be within ϵ_H as found in Propositions VI.1 and VI.2. Assuming a scenario when $\|Q\|_2\|Q^+\|_2 = \frac{\|Q\|_2}{\sigma_{\min}(Q)} = \kappa_Q \in O(1)$, $\|Y\|_2 \in O(\sqrt{d})$, $\|Q\|_2 \in \Omega(\sqrt{d})$,

we upper bound ϵ_H^{-1} with respect to m , d and ϵ as follows:

$$\epsilon_H \geq \min \left(\frac{\min(\sigma_{\min}(Q), \sigma_{\min}(\hat{Q}))}{\sqrt{\min(m, d)md}}, \frac{\epsilon}{6\sqrt{m}\|Y\|_2\|Q\|_2\|Q^+\|_2^2} \right) \quad (25)$$

$$\Rightarrow \frac{1}{\epsilon_H} \leq \max \left(\frac{\sqrt{\min(m, d)md}}{\min(\sigma_{\min}(Q), \sigma_{\min}(\hat{Q}))}, \frac{6\sqrt{m}\|Y\|_2\|Q\|_2\|Q^+\|_2^2}{\epsilon} \right) \quad (26)$$

$$\Rightarrow \frac{1}{\epsilon_H} \in \max \left(O(m), O\left(\frac{\sqrt{m}}{\epsilon}\right) \right) \in O\left(\frac{m}{\epsilon}\right) \quad (27)$$

Combining the results in Propositions VI.1 and VI.2, if we want the final loss term of our hybrid quantum-classical model to have an error within ϵ , then the total number of measurements needed falls within the complexity of

$$t \in O\left(\frac{m^3 d}{\epsilon^2} \log \frac{md}{\delta}\right) \quad (28)$$

for the probability of $1 - \delta$ using direct measurements, and

$$t \in O\left(\frac{m^2 p d \max_{k \in [q]} \|O_k\|_S^2}{\epsilon^2} \log \frac{md}{\delta}\right) \quad (29)$$

using the classical shadows protocol.

Given that we have found the number of measurements needed for a (p, q) -hybrid strategy for linear regression problems, we compare the number of measurements needed for different design principles for post-variational methods in Table I.

Alternatively, we can discuss the effects of transforming the above problem into a classification task via logistic regression, which is done by simply adding a sigmoid function in between the weighted sum and the final output with $y_i \in \{0, 1\}$. We refer to Appendix C for this discussion.

VII. IMPLEMENTATION AND EMPIRICAL RESULTS

In this section, we discuss the implementation details of our post-variational quantum neural network in the setting of machine learning applications. We use the `scikit-learn` library [35] for classical preprocessing, `pennylane` [36] for quantum embedding generation, and `pytorch` [37] with `pytorch-lightning`[38] for training the tunable classical model.

For our experiments, we focus on tasks that require only a small number of qubits. To do so, we first compress our classical data using dimension reduction methods such as principal component analysis (PCA) [39] in order to encode the data into a quantum state. We focus our experimental results on image classification of image data as the dimension reduction of such data can

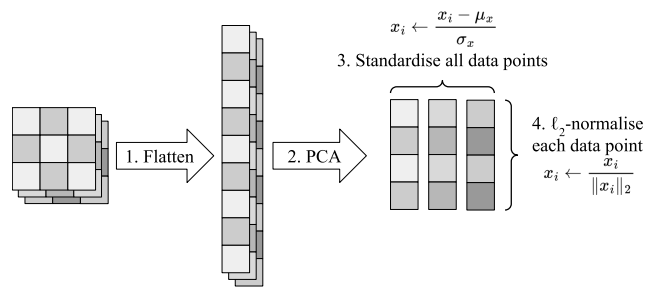


FIG. 8. Preprocessing steps for images. The image data is first flattened from a 2D tensor to a vector. Dimension reduction is then performed on the image vector to produce an image embedding. Normalization is then performed for each feature in the embedding across all data. Lastly, each vector is normalized into a unit vector to be encoded into a quantum state via amplitude encoding.

Algorithm 1 Image preprocessing

Input: Dataset $\mathcal{D} = \{x_1, x_2, \dots, x_d\}$ with images of fixed size $h \times w$, Input dimension to post-variational encoder ℓ
Output: Dataset of vectors of length m for each image $\mathcal{D}' = \{x'_1, x'_2, \dots, x'_d\}$

- 1: $\mathcal{D} \leftarrow \text{Flatten}(\mathcal{D})$ ▷ Dimensions: $d \times (hw)$
- 2: $\mathcal{D} \leftarrow \text{PCA}(\mathcal{D}, \ell)$ ▷ Dimensions: $d \times \ell$
- 3: **for** $i \leftarrow 1$ to d **do**
- 4: $x_i \leftarrow (x_i - \mu_{\mathcal{D}}) / \sigma_{\mathcal{D}}$
- 5: $x_i \leftarrow x_i / \|x_i\|_2$
- 6: **end for**
- 7: **return** \mathcal{D}

be performed directly, either by utilizing classical dimension reduction techniques on data or leveraging image compression techniques such as max or average pooling.

For the tasks that utilize other types of data such as natural language processing, we expect our strategies to be applicable, but computationally-cheap classical preprocessing would have to be conducted to produce such results. For example, to generate sentence embeddings, one possible computationally-cheap method would be to take the average pooling of the GloVe embeddings [40] of each word, and then perform dimension reduction. Hence, for simplicity, we only discuss the applications of image classification in this paper.

Problem setup and implementation details To demonstrate applicability on real-world data, we train our post-variational algorithm on the classification task based on the MNIST dataset [41], which consists of 60,000 images of size 28×28 of handwritten numbers from 0 to 9. To input the data into our quantum circuit, we follow Huang *et al.* [42] and reduce the dimension of the data into a smaller vector using PCA. Refer to Algorithm 1 and Figure 8 for exact preprocessing details.

We then produce post-variational embeddings of the input data by following the high-level outline of Algorithm 2 for observable construction constructions and

TABLE I. Upper bounds for the number of measurements for the different design principles of post-variational methods. The better approach between direct measurement and classical shadows for different design principles is bolded. Given that the Ansatz expansion strategy does not employ multiple observables, the classical shadows method does not provide a speedup, and direct measurement should be used. For the observation construction and hybrid strategy, classical shadows provide a speedup only when the measurement observables are local.

p Ansätze, q observables, n qubits, d data points	Direct measurement	Classical shadows
Ansatz expansion ($q = 1$)	$O\left(\frac{p^3 d}{\epsilon^2} \log \frac{pd}{\delta}\right)$	$O\left(\frac{p^3 d \ O\ _S^2}{\epsilon^2} \log \frac{pd}{\delta}\right)$
Observable construction ($p = 1$)	$O\left(\frac{q^3 d}{\epsilon^2} \log \frac{qd}{\delta}\right)$	$O\left(\frac{q^2 d \max_{k \in [q]} \ O\ _S^2}{\epsilon^2} \log \frac{qd}{\delta}\right)$
Hybrid	$O\left(\frac{m^3 d}{\epsilon^2} \log \frac{qd}{\delta}\right)$	$O\left(\frac{m^2 pd \max_{k \in [q]} \ O\ _S^2}{\epsilon^2} \log \frac{md}{\delta}\right)$
\mathcal{K} -local observable construction ($q \in O(3^\mathcal{K} n^\mathcal{K}), p = 1$)	$O\left(\frac{27^\mathcal{K} n^{3\mathcal{K}} \mathcal{K} d}{\epsilon^2} \log \frac{nd}{\delta}\right)$	$O\left(\frac{27^\mathcal{K} n^{2\mathcal{K}} \mathcal{K} d}{\epsilon^2} \log \frac{nd}{\delta}\right)$
\mathcal{K} -local Hybrid ($q \in O(3^\mathcal{K} n^\mathcal{K})$)	$O\left(\frac{27^\mathcal{K} n^{3\mathcal{K}} \mathcal{K} pd}{\epsilon^2} \log \frac{npd}{\delta}\right)$	$O\left(\frac{27^\mathcal{K} n^{2\mathcal{K}} \mathcal{K} pd}{\epsilon^2} \log \frac{npd}{\delta}\right)$

Algorithm 2 Observable construction Embedding Generation

Input: Dataset of vectors of length ℓ for each image $\mathcal{D} = \{x_1, x_2, \dots, x_d\}$, Observable List \mathcal{O}
Output: Tensor of post-variational embedding for all data
1: **for** $i \leftarrow 0$ to d **do**
2: $|x_i\rangle \leftarrow \text{QuantumEmbedding}(\mathcal{D}[i])$
3: **for** $k \leftarrow 0$ to $|\mathcal{O}|$ **do**
4: $\text{encoding}[i][k] \leftarrow \langle x_i | \mathcal{O}[k] | x_i \rangle$
5: **end for**
6: **end for**
7: **return** encoding

Algorithm 3 for Ansatz expansion and hybrid strategies. If the classical shadows protocol is used, we replace the measurement step of retrieving $\langle x_i | \mathcal{O}[k] | x_i \rangle$ in both algorithms with a classical shadows estimation generated from a set of unitaries \mathcal{U} that are either randomly chosen [43] or found by derandomized strategies [44, 45].

In particular, we set up the quantum circuit using Schuld *et al.* [21]’s variational circuit as our template, embedding the compressed data via amplitude embedding [46] such that a state $|\psi(x_i)\rangle$ is the direct vector representation of the normalized input in order to maintain enough information from the PCA preprocessing:

$$|\psi(x_i)\rangle = \frac{1}{\|x_i\|_2} (x_{i,1} \ x_{i,2} \ \dots \ x_{i,\ell})^\top. \quad (30)$$

For Ansatz expansion and hybrid approaches, we set the Ansatz to be the PennyLane’s implementation [36] of the strongly entangling layer proposed in Schuld *et al.* [21] (`qml.StronglyEntanglingLayer`), and initialize the parameters according to the strategy given by Grant *et al.* [8], which sets the initial parameters such that such Ansatz layer evaluates to identity. This strategy ensures that the first-order gradient as well as higher-order gradients can be non-trivial, which can allow the Ansatz

Algorithm 3 Ansatz expansion/Hybrid embedding generation

Input: Dataset of vectors of length ℓ for each image $\mathcal{D} = \{x_1, x_2, \dots, x_d\}$, Observable List \mathcal{O} , Maximum Derivative Order maxOrder
Output: Tensor of post-variational embedding for all data
1: **for** $i \leftarrow 0$ to d **do**
2: $|x_i\rangle \leftarrow \text{QuantumEmbedding}(\mathcal{D}[i])$
3: **for** $j \leftarrow 0$ to maxOrder **do**
4: $|x_{i,j}\rangle \leftarrow \frac{\partial^{(j)}}{\partial \theta^{(j)}} \text{Ansatz}(\theta_0) |x_i\rangle$
5: **for** $k \leftarrow 0$ to $|\mathcal{O}|$ **do**
6: $\text{encoding}[i][j][k] \leftarrow \langle x_{i,j} | \mathcal{O}[k] | x_{i,j} \rangle$
7: **end for**
8: **end for**
9: $\text{encoding}[i] \leftarrow \text{Flatten}(\text{encoding}[i])$
10: **end for**
11: **return** encoding

expansion technique to avoid barren plateaus. Furthermore, as the evaluation of the parameterized gates is the identity, we can ensure that the hybrid approach is at least as powerful as the observable construction approach as setting the Ansatz to identity reduces to the observable construction approach. We dub this Ansatz the “*Identity Origin Strongly Entangling Ansatz*”.

Referring to Figure 9, we combine two layers of Schuld *et al.* [21]’s Ansatz layer to form an Ansatz block that can evaluate to identity by setting initializing all parameters to 0. This Ansatz block can be further stacked alongside applying changes to the controlled gates’ orientation and range to create a deeper and more complex model, but in our experiments, we use a single layer for simplicity and to maintain the shallowness of our circuits.

Experimental setup For ease of training and benchmarking, we train our model on 2000 samples of the digits 0 and 1 in the MNIST dataset and test on 200 samples. For all experiments, the quantum embedding is the di-

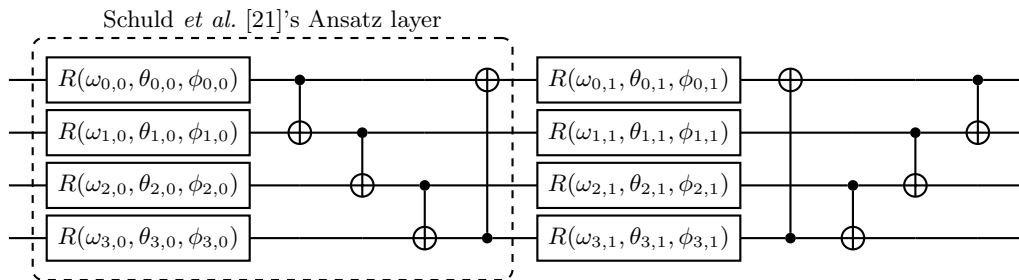


FIG. 9. The identity origin strongly entangling Ansatz. This ansatz block combines two layers of Schuld *et al.* [21]’s strongly entangled Ansatz in order to be initialized to identity by setting all parameters to be 0 per Grant *et al.* [8]’s strategy to avoid barren plateaus by initialization of parameters.

TABLE II. Effectiveness of locality constraints of the observable construction strategy. We note that empirical results show that taking an ensemble local Paulis do indeed serve as a valid approximation heuristic, with 3-local observables achieving 96% accuracy.

Locality	Validation			Testing		
	Loss	Accuracy	F1	Loss	Accuracy	F1
1	0.67	0.56	0.60	0.67	0.58	0.69
2	0.40	0.83	0.82	0.42	0.82	0.82
3	0.10	0.96	0.96	0.11	0.96	0.96

rect amplitude embedding of the dimension-reduced image on 8 qubits. Following Schuld *et al.* [21], we conduct training using k -fold cross validation [47] with $k = 5$. For the classical model, we use a simple linear classifier that trains for 150 epochs with an AdamW optimizer [48] with a learning rate of 10^{-3} . Model selection based on the highest validation F1 score is applied to prevent overfitting. For experimental results, the results refer to that which is trained on the expected value of outputs from the quantum encoders based on classical simulations by PennyLane, that is, we do not include the occurrence of measurement errors.

Experimental results We first experiment on the effectiveness of the locality constraint on the observable construction strategy for constructing post-variational quantum circuits. (Table II). We find that with just a locality of 3, the algorithm can achieve an accuracy of 96% on both validation and testing results, indicating that ensembling local Pauli observables is indeed a good heuristic for the observable construction strategy and may potentially be extended beyond the distribution restrictions in Huang *et al.* [30]’s theoretical guarantees.

On the other hand, we find that the hybrid method produces better training results compared to the observable construction strategy. Recall the hybrid method uses is at least as powerful as the observable construction strategy with our Ansatz design. Taking only the first-order derivative into account and a locality restriction of 2 for both the hybrid and observable construction strategy while applying a simple computational measurement on the first qubit for the Ansatz expansion strategy,

TABLE III. Effectiveness of different design principles of post-variational neural networks. We note that even with a 2-local system, the hybrid strategy is already able to achieve results similar to variational algorithms.

Strategy	Validation			Testing		
	Loss	Accuracy	F1	Loss	Accuracy	F1
Ansatz	0.70	0.49	0.57	0.69	0.50	0.66
Observable	0.40	0.83	0.82	0.42	0.82	0.82
Hybrid	0.15	0.94	0.94	0.20	0.91	0.90
Variational [21]	-	0.97	-	-	-	-

TABLE IV. Training results of multiclass classification. Post-variational algorithms have the extended benefit of employing a single model to conduct multi-class classification task, where as variational algorithms are restricted to binary outputs.

Class	0	1	2	3	4	5	6	7	8	9	Macro Avg
F1 Score	.88	.97	.81	.76	.79	.75	.86	.83	.74	.79	.82

we note that the addition of the first-order derivative gives an 8% increase in accuracy for the measurement observable set with locality 2. (Table III) Note that the Ansatz expansion approach is effectively the variational algorithm with only parameter tuning of one iteration and has roughly the same performance as random guessing. Comparing the training results on variational algorithms obtained by Schuld *et al.* [21] as noted in Li *et al.* [49], we see that even with a 2-local set of Ansätze and observables, the post-variational method can achieve similar performances to that of variational algorithms by use of our hybrid strategy. We expect such results to improve as we take higher-order derivatives, observables of higher locality, and more complex neural network models.

Finally, we mention the capacities of such models in the training of multiclass data, which is not directly achievable by variational algorithms as their outcomes are binary. Training on the full MNIST dataset on the same configurations, we find that we can achieve 82% accuracy on the observable construction approach with a locality of 3. (Table IV)

VIII. CONCLUSION

The large-scale realization of quantum computing is largely limited by the development of relevant hardware. With the requirement of millions of physical qubits to simulate thousands of logical qubits due to the need for quantum correction codes, a current strategy lies in hybrid computation with both classical and near-term quantum computers. Variational algorithms, one of the strategies for quantum computing in the NISQ era, are affected by the barren plateau problem, restricting the applicability of gradient-based optimizations with quantum neural networks.

This paper proposes “*post-variational strategies*” on hybrid quantum-classical devices that shift tunable parameters from quantum computers to classical computers, utilizing quantum computers to create multiple weak quantum encoders whose result can be sent into classical models to produce a class of hybrid quantum-classical algorithms, while still being rooted in the theoretical basis of the variational method for finding approximations in quantum mechanics.

We have shown that the post-variational strategies can be utilized with neural networks, and require duplicate measurements to worst case, approximately the square

of the number of quantum feature maps used, to minimize the propagation of estimation errors to the classical neural network within an arbitrarily small error rate.

Furthermore, by utilizing a hybrid strategy of using both small-order expansions of parameterized Ansätze and a series of local Pauli measurements to construct quantum circuits, we can empirically show that the post-variational algorithms are indeed applicable to machine learning problems such as image classification with high accuracy.

ACKNOWLEDGMENTS

This work is modified from and was performed in the context of a Bachelor of Computing Dissertation at the National University of Singapore. The authors would like to thank Dr. Rahul Jain, Dr. Warut Suksompong, Beng Yee Gan, Naixu Guo, and Xiufan Li for their insightful comments and discussions in the review of this work. This research is supported by the National Research Foundation, Singapore, and A*STAR under its CQT Bridging Grant and its Quantum Engineering Programme under grant NRF2021-QEP2-02-P05.

Appendix A: Deconstruction of a variational Ansatz

Here we provide a simple argument to deconstruct a variational Ansatz and show that given enough terms, the post-variational algorithm can retrieve the optimum obtained by the variational Ansatz with a terminable guarantee.

As quantum circuits are specified by a sequential arrangement of quantum logic gates, the variational ansatz $U(\theta)$ of a variational quantum circuit that is parameterized by $\theta \in \mathbb{R}^s$ can be expressed as a product of unitaries such that

$$U(\theta) = U_1(\theta_1)U_2(\theta_2) \cdots U_s(\theta_s). \quad (\text{A1})$$

For the sake of simplicity, we discuss only one-parameter quantum logic gates for our analysis of the variational algorithm.

Theorem A.1 (Stone’s theorem on one-parameter unitary groups [50, 51]). *A one-to-one correspondence between Hermitian operators H on a Hilbert space $\mathcal{H} = \mathbb{C}^{2^n}$ and one-parameter families $(U_t)_{t \in \mathbb{R}}$ of strongly continuous homomorphic unitaries can be shown as follows:*

$$U_t = e^{itH}.$$

Formally, the variational ansatz $U(\theta)$ can be expanded using Stone’s theorem as,

$$U(\theta) = W_1 e^{i\theta_1 H_1} V_1 W_2 e^{i\theta_2 H_2} V_2 \cdots W_s e^{i\theta_s H_s} V_s. \quad (\text{A2})$$

where W_i and V_i are fixed unitaries and H_i are Hermitian operators.

Proposition A.2 (Baker–Campbell–Hausdorff identity [52]). *Given two matrices X and Y ,*

$$e^X Y e^{-X} = \sum_{n=0}^{\infty} \frac{[(X)^n, Y]}{n!},$$

where $[(X)^n, Y] \equiv \underbrace{[X, \cdots [X, [X, Y]]}_{n \text{ times}}$ and $[(X)^0, Y] \equiv Y$.

We apply this identity recursively to rewrite the Hermitian operator $U^\dagger(\theta)OU(\theta)$ in polynomial terms of $\theta_1, \theta_2, \dots, \theta_s$. Expanding the first unitary U_1 , we get

$$U_1^\dagger(\theta_1)OU_1(\theta_1) = V_1^\dagger \left(\sum_{k=0}^{\infty} \frac{[(i\theta_1 H_1)^k, W_1^\dagger O W_1]}{k!} \right) V_1 = \sum_{k=0}^{\infty} \frac{\theta_1^k}{k!} V_1^\dagger [(iH_1)^k, W_1^\dagger O W_1] V_1. \quad (\text{A3})$$

We note that the term iH_j is anti-Hermitian, hence for all $k \geq 0$, $V_1^\dagger [(iH_1)^k, W_1^\dagger O W_1] V_1$ is Hermitian. Thus, we can write $U_1^\dagger(\theta_1)OU_1(\theta_1)$ as a weighted polynomial sum of Hermitians against θ_1 . Plugging the result recursively against the other terms, one can obtain

$$U^\dagger(\theta)OU(\theta) = \sum_{0 \leq a_1, a_2, \dots, a_s \leq \infty} \frac{\theta_1^{a_1}}{a_1!} \frac{\theta_2^{a_2}}{a_2!} \dots \frac{\theta_s^{a_s}}{a_s!} \underbrace{V_s^\dagger [(iH_s)^{a_s}, W_s^\dagger V_{s-1}^\dagger [(iH_{s-1})^{a_{s-1}}, W_{s-1}^\dagger V_{s-2}^\dagger [\dots, V_1^\dagger [(iH_1)^k, W_1^\dagger O W_1] V_1 W_2] \dots] V_{s-1} W_s] V_s}_{\text{Hermitian}}. \quad (\text{A4})$$

This expansion allows one to express

$$\mathcal{O}(\theta) = U(\theta)OU^\dagger(\theta) \approx \sum_i \mathcal{F}_i(\theta) \mathcal{O}_i. \quad (\text{A5})$$

This discussion shows that a deconstruction of the variational algorithm does indeed exist formally and corresponds to a linear combination of Hermitians. However, we note that there are currently infinite terms in this expression. We now show that we can express this linear combination in limited terms. Any Hermitian operator can be expressed in a basis of Pauli matrices such that

$$H \in (\mathbb{C}^2)^{\otimes n} \rightarrow H \in \text{span}(\{\mathcal{I}, \mathcal{X}, \mathcal{Y}, \mathcal{Z}\}^{\otimes n}), \quad (\text{A6})$$

hence, we can state that

$$U^\dagger(\theta)OU(\theta) \in \text{span}(\{\mathcal{I}, \mathcal{X}, \mathcal{Y}, \mathcal{Z}\}^{\otimes n}), \quad (\text{A7})$$

where each coefficient is $\text{poly}(\theta_1, \theta_2, \dots, \theta_s)$.

Therefore, supposing that the variational algorithm obtains an optimal θ^* , the post-variational algorithm requires at most 4^n terms to express the same optimal answer. Comparing the number of parameters tunable, we see that the variational algorithm requires $O(\text{poly}(s))$ parameters, while the post-variational algorithm requires $O(4^n)$ parameters. We note that the quantum advantage of variational algorithms in terms of parameters is the ability to generate different observables on higher orders of θ , a feat that activation functions of classical computers cannot achieve, as classical activation functions can only non-linearize the θ parameter itself without generating new observables. However, considering that the variational algorithm returns an estimation of the optimal answer, rather than the exact optimal answer, we hope to restrict the number of Hermitian terms used in the post-variational algorithm to $O(\text{poly}(s))$ terms to achieve a similar estimation.

Appendix B: Derivation of random measurement errors

Proof of Proposition VI.1. We represent the output of a single quantum neuron over a single data output over multiple runs as a series of i.i.d. random variables Z_1, Z_2, \dots, Z_t , each with a range of $[-1, 1]$. Then by Hoeffding bound [33], we find that the sample mean \bar{Z} and the expectation of the above random variables have $\Pr(|\bar{Z} - E[Z]| \geq \epsilon) \leq 2 \exp(-\frac{t\epsilon^2}{2})$. Further, as each run is associated with a single data point on a single quantum neuron, we need to apply a union bound [34] to ensure for all m quantum neurons, and d data points, we only have a small probability of $|\bar{Z} - E[Z]| \geq \epsilon_H$. We denote the event $E_{i,j}$ as the observation i th data point and j th quantum neuron having $|\bar{Z} - E[Z]| \geq \epsilon_H$ for the corresponding observations. We then see that $\Pr(\cup_{i=1}^m \cup_{j=1}^d E_{i,j}) \leq \sum_{i=1}^m \sum_{j=1}^d \Pr(E_{i,j}) = md \cdot \Pr(|\bar{Z} - E[Z]| \geq \epsilon_H) \leq 2md \exp(-\frac{t\epsilon_H^2}{2}) \leq \delta$, such that $t \in O(\frac{1}{\epsilon_H} \log \frac{md}{\delta})$. We note the number of quantum measurements are duplicated across m quantum neurons and d data points, hence the total number of observations required is $O(\frac{md}{\epsilon_H} \log \frac{md}{\delta})$. \square

Proof of Proposition VI.2. For simplicity, we consider the original classical shadows protocol [16] utilizing the median-of-means estimator [19] for discussion. With the median-of-means estimator, one partitions the number of measurements into s groups of t measurements, taking the median of the mean over the t measurements from the s groups. From the analysis of the median-of-means estimator in [16], we note that with probability $1 - \delta$, per Hoeffding bound [33] and Chebyshev's inequality, one should set $t \in O(\frac{\max_{k \in [q]} \|O_k\|_S^2}{\epsilon^2})$ and per union bound, one should set $s \in O(\log \frac{md}{\delta})$. As the classical shadows method predicts the outcome of q quantum neurons that share the same Ansatz and data point, the process has to be duplicated over d data points and p different Ansätze. Hence the total number of measurements needed in total is then $O\left(\frac{pd \max_{k \in [q]} \|O_k\|_S^2}{\epsilon_H^2} \log \frac{md}{\delta}\right)$. \square

Appendix C: Derivation of error propagation

In this section, we detail the derivation of the error propagation of the element-wise error of the quantum neuron to the entire network. Before the proofs, we first set up some further notations needed./ Given a field \mathbb{F} of either real or complex numbers, for matrix $A \in \mathbb{F}^{M \times N}$, we denote the Frobenius norm, or Hilbert-Schmidt norm, to be $\|A\|_F = \sqrt{\sum_i \sum_j |A_{ij}|^2} = \sqrt{\sum_{i=1}^{\min(M,N)} \sigma_i^2(A)}$. We also denote the nuclear norm to be $\|A\|_* = \sum_{i=1}^{\min(M,N)} \sigma_i(A)$. Recall that $\sigma_i(A)$ is the i -th singular value of A .

Before we prove Theorem VI.3, we first show some preliminaries to aid the proof of our results. For matrix $A \in \mathbb{R}^{M \times N}$, we note the following inequalities for matrix norms

$$\|A\|_{\max} \leq \|A\|_2 \leq \|A\|_F \leq \sqrt{MN} \|A\|_{\max}, \quad (\text{C1})$$

$$\|A\|_F \leq \|A\|_* \leq \sqrt{r} \|A\|_F \leq r \|A\|_2, \quad (\text{C2})$$

where $r = \text{rank}(A) \leq \min(M, N)$.

Proposition C.1 (Perturbation inequality for concave functions of singular values [53, 54]). *Given matrices $A, B \in \mathbb{R}^{M \times N}$. Suppose that $f : \mathbb{R}_+ \rightarrow \mathbb{R}_+$ is a concave function where $f(0) = 0$, then we have*

$$\sum_{i=1}^{\min(M,N)} |f(\sigma_i(A)) - f(\sigma_i(B))| \leq \sum_{i=1}^{\min(M,N)} f(\sigma_i(A - B)).$$

We use this proposition to prove the follow lemma.

Lemma C.2 (Perturbation inequality for rank differences). *Given matrix $A, B \in \mathbb{R}^{M \times N}$, if $\|A - B\|_{\max} < \min(\sigma_{\min}(A), \sigma_{\min}(B)) / \sqrt{\min(M, N)MN}$, where $\sigma_{\min}(A)$ is the smallest non-zero singular value of A , then $\text{rank}(A) = \text{rank}(B)$.*

Proof. We define concave function $f_\mu : \mathbb{R}_+ \rightarrow [0, 1]$ such that

$$f_\mu(x) := \begin{cases} \frac{x}{\mu}, & 0 \leq x < \mu, \\ 1, & \mu \leq x. \end{cases} \quad (\text{C3})$$

Suppose that $\mu = \min(\sigma_{\min}(A), \sigma_{\min}(B))$, we find that

$$\sum_{i=1}^{\min(M,N)} |f_\mu(\sigma_i(A)) - f_\mu(\sigma_i(B))| = |\text{rank}(A) - \text{rank}(B)|. \quad (\text{C4})$$

Then by Proposition C.1, we see that

$$|\text{rank}(A) - \text{rank}(B)| \leq \sum_{i=1}^{\min(M,N)} f_\mu(\sigma_i(A - B)) \leq \sum_{i=1}^{\min(M,N)} \frac{\sigma_i(A - B)}{\mu} = \frac{\|A - B\|_*}{\min(\sigma_{\min}(A), \sigma_{\min}(B))} \quad (\text{C5})$$

Using the matrix norm inequalities, we see that

$$|\text{rank}(A) - \text{rank}(B)| \leq \frac{\|A - B\|_*}{\min(\sigma_{\min}(A), \sigma_{\min}(B))} \leq \frac{\sqrt{\min(M, N)}\|A - B\|_F}{\min(\sigma_{\min}(A), \sigma_{\min}(B))} \leq \frac{\sqrt{\min(M, N)MN}\|A - B\|_{\max}}{\min(\sigma_{\min}(A), \sigma_{\min}(B))} \quad (\text{C6})$$

Setting an upper bound of 1 for the above inequality, we find that if $\frac{\sqrt{\min(M, N)MN}\|A - B\|_{\max}}{\min(\sigma_{\min}(A), \sigma_{\min}(B))} < 1$, or

$$\|A - B\|_{\max} < \frac{\min(\sigma_{\min}(A), \sigma_{\min}(B))}{\sqrt{\min(M, N)MN}}, \quad (\text{C7})$$

then $|\text{rank}(A) - \text{rank}(B)| < 1$. Given that ranks have positive integers values, we find that $\text{rank}(A) = \text{rank}(B)$. \square

We also use the following proposition:

Proposition C.3 (Perturbation theory For pseudoinverses [55]). *The spectral norm of the difference of the pseudoinverses of two matrices $A \in \mathbb{R}^{m \times n}$ and $B \in \mathbb{R}^{m \times n}$ can be upper bounded as follows if $\text{rank}(A) = \text{rank}(B)$:*

$$\|B^+ - A^+\|_2 \leq 2\|A^+\|_2\|B^+\|_2\|B - A\|_2.$$

We continue with putting these technical results together to prove the Theorem VI.3 of the main text.

Proof of Theorem VI.3. Recall that

$$\Delta\mathcal{L}_{\text{RMSE}} = |\mathcal{L}_{\text{RMSE}}(\hat{\alpha}^*, Q) - \mathcal{L}_{\text{RMSE}}(\alpha^*, Q)|. \quad (\text{C8})$$

Expanding directly, we obtain

$$\Delta\mathcal{L}_{\text{RMSE}} = \frac{1}{\sqrt{d}} \|\|Y - Q\hat{\alpha}^*\|_2 - \|Y - Q\alpha^*\|_2\| \quad (\text{C9})$$

$$\text{(reverse triangle)} \leq \frac{1}{\sqrt{d}} \|Q(\hat{\alpha}^* - \alpha^*)\|_2 \leq \frac{1}{\sqrt{d}} \|Q\|_2 \|\hat{\alpha}^* - \alpha^*\|_2 \quad (\text{C10})$$

$$= \frac{1}{\sqrt{d}} \|Q\|_2 \|\hat{Q}^+ Y - Q^+ Y\|_2 \leq \frac{1}{\sqrt{d}} \|Q\|_2 \|Y\|_2 \|\hat{Q}^+ - Q^+\|_2. \quad (\text{C11})$$

With $0 < \epsilon_0 < 1$, we conduct enough measurements such that $\|\hat{Q} - Q\|_{\max} < \epsilon_0 \frac{\min(\sigma_{\min}(Q), \sigma_{\min}(\hat{Q}))}{\sqrt{\min(m, d)md}}$, hence by Lemma C.2, $\text{rank}(Q) = \text{rank}(\hat{Q})$. Then by Proposition C.3, we obtain

$$\|\hat{Q}^+ - Q^+\|_2 \leq 2\|Q^+\|_2\|\hat{Q}^+\|_2\|\hat{Q} - Q\|_2 \leq 2\|Q^+\|_2 \left(\|Q^+\|_2 + \|\hat{Q}^+ - Q^+\|_2 \right) \|\hat{Q} - Q\|_2 \quad (\text{C12})$$

$$\Rightarrow \|\hat{Q}^+ - Q^+\|_2 \leq \frac{2\|Q^+\|_2^2\|\hat{Q} - Q\|_2}{1 - 2\|Q^+\|_2\|\hat{Q} - Q\|_2}. \quad (\text{C13})$$

We note that if $m, d \geq 9$, then

$$\|Q^+\|_2\|\hat{Q} - Q\|_2 \leq \frac{\sqrt{md}}{\sigma_{\min}(Q)} \|\hat{Q} - Q\|_{\max} < \frac{\sqrt{md}}{\sigma_{\min}(Q)} \frac{\min(\sigma_{\min}(Q), \sigma_{\min}(\hat{Q}))}{\sqrt{\min(m, d)md}} \leq \frac{1}{\sqrt{\min(m, d)}} \leq \frac{1}{3}. \quad (\text{C14})$$

Hence we see that

$$\|\hat{Q}^+ - Q^+\|_2 \leq 6\|Q^+\|_2^2\|\hat{Q} - Q\|_2. \quad (\text{C15})$$

Evaluating the loss

$$\Delta\mathcal{L}_{\text{RMSE}} < \frac{6}{\sqrt{d}} \|Y\|_2 \|Q\|_2 \|Q^+\|_2^2 \|\hat{Q} - Q\|_2 \leq \frac{6\sqrt{md}}{\sqrt{d}} \|Y\|_2 \|Q\|_2 \|Q^+\|_2^2 \|\hat{Q} - Q\|_{\max} \quad (\text{C16})$$

$$< 6\|Y\|_2 \|Q\|_2 \|Q^+\|_2^2 \frac{\min(\sigma_{\min}(Q), \sigma_{\min}(\hat{Q}))}{\sqrt{\min(m, d)d}} \epsilon_0. \quad (\text{C17})$$

Now setting (it has to satisfy the upper bound 1)

$$\epsilon_0 \leq \min \left(1, \frac{\epsilon \sqrt{\min(m, d)d}}{6\|Y\|_2 \|Q\|_2 \|Q^+\|_2^2 \min(\sigma_{\min}(Q), \sigma_{\min}(\hat{Q}))} \right), \quad (\text{C18})$$

then $\Delta\mathcal{L}_{\text{RMSE}} \leq \epsilon$. We hence obtain for element-wise bound

$$\|\hat{Q} - Q\|_{\max} < \epsilon_0 \frac{\min(\sigma_{\min}(Q), \sigma_{\min}(\hat{Q}))}{\sqrt{\min(m, d)m\bar{d}}} \leq \min\left(\frac{\min(\sigma_{\min}(Q), \sigma_{\min}(\hat{Q}))}{\sqrt{\min(m, d)m\bar{d}}}, \frac{\epsilon}{6\sqrt{m}\|Y\|_2\|Q\|_2\|Q^+\|_2^2}\right). \quad (\text{C19})$$

□

Lastly, we discuss the error analysis of logistic regression problems. Consider the following formulation of the logistic regression problem: For all data points in $\mathcal{D} = \{(x_i, y_i)\}_{i=1}^d$, the binary outcome Y_i for point x_i can be described as a Bernoulli-sampled data such that

$$Y_i|x_i \sim \text{Bernoulli}(p_i). \quad (\text{C20})$$

Here, p_i is the i -dependent parameter of the Bernoulli distribution. One can then see that:

$$\mathbb{E}[Y_i|x_i] = p_i. \quad (\text{C21})$$

Given the formulation of logistic regression as a generalized linear model, we note that α is learned such that

$$\text{logit}(\mathbb{E}[Y_i|x_i]) = \frac{p_i}{1-p_i} = \alpha \cdot x_i \quad (\text{C22})$$

$$\text{logit}(\mathbb{E}[Y_i|\hat{x}_i]) = \frac{\hat{p}_i}{1-\hat{p}_i} = \hat{\alpha} \cdot \hat{x}_i \quad (\text{C23})$$

Denoting $L = \left(\frac{p_1}{1-p_1}, \frac{p_2}{1-p_2}, \dots, \frac{p_d}{1-p_d}\right)^\top$, and $\hat{L} = \left(\frac{\hat{p}_1}{1-\hat{p}_1}, \frac{\hat{p}_2}{1-\hat{p}_2}, \dots, \frac{\hat{p}_d}{1-\hat{p}_d}\right)^\top$, we can see that by least squares solution to the above problem, $\alpha^* = Q^+L$ and $\hat{\alpha}^* = \hat{Q}^+\hat{L}$. Now recall that

$$\Delta\mathcal{L}_{\text{BCE}} = |\mathcal{L}_{\text{BCE}}(\hat{\alpha}^*, Q) - \mathcal{L}_{\text{BCE}}(\alpha^*, Q)| \quad (\text{C24})$$

$$\begin{aligned} &= \frac{1}{d} \sum_{i=1}^d y_i \left| \log\left(\sigma\left(\sum_{j=1}^m \hat{\alpha}_j^* Q_{ij}\right)\right) - \log\left(\sigma\left(\sum_{j=1}^m \alpha_j^* Q_{ij}\right)\right) \right| \\ &\quad + (1-y_i) \left| \log\left(1 - \sigma\left(\sum_{j=1}^m \hat{\alpha}_j^* Q_{ij}\right)\right) - \log\left(1 - \sigma\left(\sum_{j=1}^m \alpha_j^* Q_{ij}\right)\right) \right| \end{aligned} \quad (\text{C25})$$

We observe that the functions $\log(\sigma(\cdot))$ and $\log(1 - \sigma(\cdot))$ are Lipschitz continuous, with the Lipschitz constant being

$$K_{\log(\sigma(\cdot))} = \sup_{x \in \mathbb{R}} \left| \frac{\partial \log(\sigma(x))}{\partial x} \right| = \sup_{x \in \mathbb{R}} (1 - \sigma(x)) = 1, \quad (\text{C26})$$

$$K_{\log(1-\sigma(\cdot))} = \sup_{x \in \mathbb{R}} \left| \frac{\partial \log(1 - \sigma(x))}{\partial x} \right| = \sup_{x \in \mathbb{R}} \sigma(x) = 1. \quad (\text{C27})$$

Hence, we see that

$$\Delta\mathcal{L}_{\text{BCE}} \leq \frac{1}{d} \sum_{i=1}^d y_i \left| \sum_{j=1}^m \hat{\alpha}_j^* Q_{ij} - \sum_{j=1}^m \alpha_j^* Q_{ij} \right| + (1-y_i) \left| \sum_{j=1}^m \hat{\alpha}_j^* Q_{ij} - \sum_{j=1}^m \alpha_j^* Q_{ij} \right| \quad (\text{C28})$$

$$= \frac{1}{d} \sum_{i=1}^d \left| \sum_{j=1}^m \hat{\alpha}_j^* Q_{ij} - \sum_{j=1}^m \alpha_j^* Q_{ij} \right| = \frac{1}{d} \|Q\hat{\alpha}^* - Q\alpha^*\|_1 \leq \frac{1}{\sqrt{d}} \|Q\hat{\alpha}^* - Q\alpha^*\|_2. \quad (\text{C29})$$

Plugging in the least square solutions of α^* and $\hat{\alpha}^*$, we obtain

$$\Delta\mathcal{L}_{\text{BCE}} \leq \frac{1}{\sqrt{d}} \|Q\hat{\alpha}^* - Q\alpha^*\|_2 \leq \frac{1}{\sqrt{d}} \|Q\|_2 \|\hat{Q}^+\hat{L} - Q^+L\|_2 \leq \frac{1}{\sqrt{d}} \|Q\|_2 \|L\|_2 \|\hat{Q}^+ - Q^+\|_2 + \frac{1}{\sqrt{d}} \|Q\|_2 \|\hat{Q}^+\|_2 \|\hat{L} - L\|_2. \quad (\text{C30})$$

We note that the first term is the RMSE loss for linear systems when $Y = L$. We note that as p_i and \hat{p}_i are unknown and hence one cannot evaluate the term of $\|\hat{L} - L\|_2$. We note that from Theorem VI.3, we obtain for element-wise bound

$$\|\hat{Q} - Q\|_{\max} < \min \left(\frac{\min(\sigma_{\min}(Q), \sigma_{\min}(\hat{Q}))}{\sqrt{\min(m, d)md}}, \frac{\epsilon}{6\sqrt{m}\|L\|_2\|Q\|_2\|Q^+\|_2^2} - \frac{\|\hat{Q}^+\|_2\|\hat{L} - L\|_2}{6\sqrt{md}\|L\|_2\|Q^+\|_2^2} \right), \quad (\text{C31})$$

the loss difference of $\Delta\mathcal{L}_{\text{BCE}} \leq \epsilon$ is satisfied.

-
- [1] M. Cerezo, A. Arrasmith, R. Babbush, S. C. Benjamin, S. Endo, K. Fujii, J. R. McClean, K. Mitarai, X. Yuan, L. Cincio, and P. J. Coles, Variational quantum algorithms, *Nature Reviews Physics* **3**, 625 (2021).
- [2] A. Peruzzo, J. McClean, P. Shadbolt, M.-H. Yung, X.-Q. Zhou, P. J. Love, A. Aspuru-Guzik, and J. L. O'Brien, A variational eigenvalue solver on a photonic quantum processor, *Nature Communications* **5** (2014).
- [3] E. Farhi, J. Goldstone, and S. Gutmann, A quantum approximate optimization algorithm (2014), arXiv:1411.4028 [quant-ph].
- [4] K. Mitarai, M. Negoro, M. Kitagawa, and K. Fujii, Quantum circuit learning, *Phys. Rev. A* **98**, 032309 (2018).
- [5] J. Preskill, Quantum Computing in the NISQ era and beyond, *Quantum* **2**, 79 (2018).
- [6] A. Kandala, A. Mezzacapo, K. Temme, M. Takita, M. Brink, J. M. Chow, and J. M. Gambetta, Hardware-efficient variational quantum eigensolver for small molecules and quantum magnets, *Nature* **549**, 242 (2017).
- [7] J. R. McClean, S. Boixo, V. N. Smelyanskiy, R. Babbush, and H. Neven, Barren plateaus in quantum neural network training landscapes, *Nature Communications* **9** (2018).
- [8] E. Grant, L. Wossnig, M. Ostaszewski, and M. Benedetti, An initialization strategy for addressing barren plateaus in parametrized quantum circuits, *Quantum* **3**, 214 (2019).
- [9] A. Skolik, J. R. McClean, M. Mohseni, P. van der Smagt, and M. Leib, Layerwise learning for quantum neural networks, *Quantum Machine Intelligence* **3** (2021).
- [10] G. Verdon, M. Broughton, J. R. McClean, K. J. Sung, R. Babbush, Z. Jiang, H. Neven, and M. Mohseni, Learning to learn with quantum neural networks via classical neural networks (2019), arXiv:1907.05415 [quant-ph].
- [11] I. Cong, S. Choi, and M. D. Lukin, Quantum convolutional neural networks, *Nature Physics* **15**, 1273 (2019).
- [12] A. Pesah, M. Cerezo, S. Wang, T. Volkoff, A. T. Sornborger, and P. J. Coles, Absence of barren plateaus in quantum convolutional neural networks, *Phys. Rev. X* **11**, 041011 (2021).
- [13] H.-Y. Huang, K. Bharti, and P. Rebentrost, Near-term quantum algorithms for linear systems of equations with regression loss functions, *New Journal of Physics* **23**, 113021 (2021).
- [14] K. Bharti and T. Haug, Iterative quantum-assisted eigensolver, *Phys. Rev. A* **104**, L050401 (2021).
- [15] K. Wan, M. Berta, and E. T. Campbell, Randomized quantum algorithm for statistical phase estimation, *Phys. Rev. Lett.* **129**, 030503 (2022).
- [16] H.-Y. Huang, R. Kueng, and J. Preskill, Predicting many properties of a quantum system from very few measurements, *Nature Physics* **16**, 1050 (2020).
- [17] R. Penrose, On best approximate solutions of linear matrix equations, *Mathematical Proceedings of the Cambridge Philosophical Society* **52**, 17–19 (1956).
- [18] D. Gottesman, *Stabilizer Codes and Quantum Error Correction*, Ph.D. thesis, Caltech (1997), arXiv:quant-ph/9705052 [quant-ph].
- [19] A. S. Nemirovsky and D. B. Yudin, *Problem complexity and method efficiency in optimization* (Wiley, 1983).
- [20] C. Bravo-Prieto, R. LaRose, M. Cerezo, Y. Subasi, L. Cincio, and P. J. Coles, Variational quantum linear solver (2020), arXiv:1909.05820 [quant-ph].
- [21] M. Schuld, A. Bocharov, K. M. Svore, and N. Wiebe, Circuit-centric quantum classifiers, *Phys. Rev. A* **101**, 032308 (2020).
- [22] E. Farhi and H. Neven, Classification with quantum neural networks on near term processors (2018), arXiv:1802.06002 [quant-ph].
- [23] M. Schuld, V. Bergholm, C. Gogolin, J. Izaac, and N. Killoran, Evaluating analytic gradients on quantum hardware, *Phys. Rev. A* **99**, 032331 (2019).
- [24] A. Pérez-Salinas, A. Cervera-Lierta, E. Gil-Fuster, and J. I. Latorre, Data re-uploading for a universal quantum classifier, *Quantum* **4**, 226 (2020).
- [25] S. Jerbi, L. J. Fiderer, H. P. Nautrup, J. M. Kübler, H. J. Briegel, and V. Dunjko, Quantum machine learning beyond kernel methods, *Nature Communications* **14** (2023).
- [26] K. Hornik, M. Stinchcombe, and H. White, Multilayer feedforward networks are universal approximators, *Neural Networks* **2**, 359 (1989).
- [27] P. Huembeli and A. Dauphin, Characterizing the loss landscape of variational quantum circuits, *Quantum Science and Technology* **6**, 025011 (2021).
- [28] A. Mari, T. R. Bromley, and N. Killoran, Estimating the gradient and higher-order derivatives on quantum hardware, *Phys. Rev. A* **103**, 012405 (2021).
- [29] M. Cerezo and P. J. Coles, Higher order derivatives of quantum neural networks with barren plateaus, *Quantum Science and Technology* **6**, 035006 (2021).
- [30] H.-Y. Huang, S. Chen, and J. Preskill, Learning to predict arbitrary quantum processes (2023), arXiv:2210.14894 [quant-ph].
- [31] M. Cerezo, A. Sone, T. Volkoff, L. Cincio, and P. J. Coles, Cost function dependent barren plateaus in shallow parametrized quantum circuits, *Nature Communications* **12** (2021).
- [32] Y. Cao, G. G. Guerreschi, and A. Aspuru-Guzik, Quantum neuron: an elementary building block for machine learning on quantum computers (2017),

- arXiv:1711.11240 [quant-ph].
- [33] W. Hoeffding, Probability inequalities for sums of bounded random variables, *Journal of the American Statistical Association* **58**, 13 (1963).
- [34] G. Boole, *The Mathematical Analysis of Logic* (Cambridge University Press, 2009).
- [35] F. Pedregosa, G. Varoquaux, A. Gramfort, V. Michel, B. Thirion, O. Grisel, M. Blondel, P. Prettenhofer, R. Weiss, V. Dubourg, J. Vanderplas, A. Passos, D. Cournapeau, M. Brucher, M. Perrot, and E. Duchesnay, Scikit-learn: Machine learning in Python, *Journal of Machine Learning Research* **12**, 2825 (2011).
- [36] V. Bergholm, J. Izaac, M. Schuld, C. Gogolin, S. Ahmed, V. Ajith, M. S. Alam, G. Alonso-Linaje, B. Akash-Narayanan, A. Asadi, J. M. Arrazola, U. Azad, S. Banning, C. Blank, T. R. Bromley, B. A. Cordier, J. Ceroni, A. Delgado, O. D. Matteo, A. Dusko, T. Garg, D. Guala, A. Hayes, R. Hill, A. Ijaz, T. Isacsson, D. Ittah, S. Jahangiri, P. Jain, E. Jiang, A. Khandelwal, K. Kottmann, R. A. Lang, C. Lee, T. Loke, A. Lowe, K. McKiernan, J. J. Meyer, J. A. Montañez-Barrera, R. Moyard, Z. Niu, L. J. O’Riordan, S. Oud, A. Panigrahi, C.-Y. Park, D. Polatajko, N. Quesada, C. Roberts, N. Sá, I. Schoch, B. Shi, S. Shu, S. Sim, A. Singh, I. Strandberg, J. Soni, A. Száva, S. Thabet, R. A. Vargas-Hernández, T. Vincent, N. Vitucci, M. Weber, D. Wierichs, R. Wiersema, M. Willmann, V. Wong, S. Zhang, and N. Killoran, PennyLane: Automatic differentiation of hybrid quantum-classical computations (2022), arXiv:1811.04968 [quant-ph].
- [37] A. Paszke, S. Gross, F. Massa, A. Lerer, J. Bradbury, G. Chanan, T. Killeen, Z. Lin, N. Gimelshein, L. Antiga, A. Desmaison, A. Kopf, E. Yang, Z. DeVito, M. Raison, A. Tejani, S. Chilamkurthy, B. Steiner, L. Fang, J. Bai, and S. Chintala, Pytorch: An imperative style, high-performance deep learning library, in *Advances in Neural Information Processing Systems 32* (Curran Associates, Inc., 2019) pp. 8024–8035.
- [38] <https://lightning.ai/pytorch-lightning>.
- [39] I. T. Jolliffe, Principal components in regression analysis, in *Principal Component Analysis* (Springer New York, 1986) pp. 129–155.
- [40] J. Pennington, R. Socher, and C. Manning, GloVe: Global vectors for word representation, in *Proceedings of the 2014 Conference on Empirical Methods in Natural Language Processing (EMNLP)* (Association for Computational Linguistics, Doha, Qatar, 2014) pp. 1532–1543.
- [41] Y. LeCun, C. Cortes, and C. J. Burges, The MNIST database (1998).
- [42] H.-Y. Huang, M. Broughton, M. Mohseni, R. Babbush, S. Boixo, H. Neven, and J. R. McClean, Power of data in quantum machine learning, *Nature Communications* **12** (2021).
- [43] A. Elben, S. T. Flammia, H.-Y. Huang, R. Kueng, J. Preskill, B. Vermersch, and P. Zoller, The randomized measurement toolbox, *Nature Reviews Physics* **5**, 9 (2022).
- [44] H.-Y. Huang, R. Kueng, and J. Preskill, Efficient estimation of pauli observables by derandomization, *Phys. Rev. Lett.* **127**, 030503 (2021).
- [45] T.-C. Yen, A. Ganeshram, and A. F. Izmaylov, Deterministic improvements of quantum measurements with grouping of compatible operators, non-local transformations, and covariance estimates, *npj Quantum Information* **9** (2023).
- [46] M. Schuld and F. Petruccione, *Supervised Learning with Quantum Computers* (Springer International Publishing, 2018).
- [47] M. Stone, Cross-validatory choice and assessment of statistical predictions, *Journal of the Royal Statistical Society. Series B (Methodological)* **36**, 111 (1974).
- [48] I. Loshchilov and F. Hutter, Decoupled weight decay regularization, in *International Conference on Learning Representations* (2019).
- [49] G. Li, Z. Song, and X. Wang, VSQL: Variational shadow quantum learning for classification, in *Proceedings of the AAAI Conference on Artificial Intelligence*, Vol. 35-9 (2021) pp. 8357–8365.
- [50] M. H. Stone, Linear transformations in hilbert space, in *Proceedings of the National Academy of Sciences*, Vol. 16-2 (1930) pp. 172–175.
- [51] M. H. Stone, On one-parameter unitary groups in hilbert space, *Annals of Mathematics* **33**, 643 (1932).
- [52] J. E. Campbell, On a law of combination of operators (second paper), in *Proceedings of the London Mathematical Society*, Vol. s1-29-1 (Wiley, 1897) pp. 14–32.
- [53] S. Oymak, K. Mohan, M. Fazel, and B. Hassibi, A simplified approach to recovery conditions for low rank matrices, in *2011 IEEE International Symposium on Information Theory Proceedings* (2011) pp. 2318–2322.
- [54] M.-C. Yue and A. M.-C. So, A perturbation inequality for concave functions of singular values and its applications in low-rank matrix recovery, *Applied and Computational Harmonic Analysis* **40**, 396 (2016).
- [55] P.-Å. Wedin, Perturbation theory for pseudo-inverses, *BIT Numerical Mathematics* **13**, 217 (1973).